Stereodynamics of ultracold rotationally inelastic collisions

Masato Morita[1, a)] and Naduvalath Balakrishnan[1, b)]
Department of Chemistry and Biochemistry, University of Nevada, Las Vegas, Nevada 89154, USA

(Dated: 3 November 2020)

Recent experiments on rotational quenching of HD in the $v = 1, j = 2$ rovibrational state in collisions with H_2, D_2 and He near 1 K have revealed strong stereodynamic preference stemming from isolated shape resonances. So far, the experiments and subsequent theoretical analyses have considered initial HD rotational state in an orientation specified by the projection quantum number m or a coherent superposition of different m states. However, it is known that such stereodynamic control is generally not effective in the ultracold energy regime due to the dominance of the incoming s-wave ($l = 0$ partial wave). Here, we provide a detailed analysis of stereodynamics of rotational quenching of HD by He with both m and m' resolution where m' refers to the inelastically scattered HD. We show the existence of significant m dependence in the m'-resolved differential and integral cross sections even in the ultracold s-wave regime with a factor greater than 60 for $j = 2 \rightarrow j' = 1$ and a factor greater than 1300 for $j = 3 \rightarrow j' = 2$ transitions. In the helicity frame, however, the integral cross section has no initial orientation (k) dependence in the ultracold energy regime even resolving with respect to final orientation (k'). The distribution of final rotational state orientations (k') is found to be statistical (uniform) regardless of the initial orientation.

I. INTRODUCTION

Cold and ultracold molecules are rapidly transforming our understanding of chemical reaction dynamics and energy transfer phenomena in the deep quantum regime. The ability to control their properties and interaction through external electric, magnetic and optical fields has led to new applications in emerging areas of quantum information processing, quantum computing, quantum sensing, and precision spectroscopy.[1–11] Ultracold chemistry experiments can offer much insights into reaction intermediates and energy dispersal as recently demonstrated for the benchmark KRb+KRb $\rightarrow$ K_2+Rb_2 reaction that was shown to occur through a four-center mechanism and a transient K_2Rb_2 intermediate complex.[12,13] Even for closed-shell molecules without an electric dipole moment (or molecules with a weak dipole moment like HD) or hyperfine structure, selective preparation of the initial molecular rotational state in an orientation specified by projection quantum number m (or a superposition of m-states) allows considerable control of angular distribution of the inelastically scattered molecule as demonstrated in recent experiments of Perreault *et al.*[14–18]

There is a long history of molecular collisions exploring the dependence of inelastic and elastic (polarization) cross sections on the projection quantum numbers m and m' of initial and final molecular rotational states.[19–31] In particular, the search for propensities $\Delta m = m' - m$ yielded new insights into collisional reorientation providing ideas for developing approximate calculation methods such as the j_z conserving coupled-states/centrifugal-sudden (CS) approximation as well as the infinite-order sudden (IOS) approximation.[23–25,29] Analogous efforts to relate dynamical outcomes to reagent approach geometry in chemical reactions (dynamical stereochemistry) have also been developed.[32–34] Nowadays, such efforts have been broadly termed as stereodynamics in which the correlation between various vector properties in collisions and reactions is examined drawing extensive research interests to deepen physical insight into the underlying dynamics.[35–45]

An experimental scheme recently proposed by Perreault *et al.*[14–16] has proved to be a powerful tool for probing stereodynamics of molecular collisions when a small number of partial waves control the collision outcome. In their intra-beam scheme, a co-expansion of colliding species in a supersonic molecular beam effectively reduces the relative collision energy to around 1 K (provided the collision partners have comparable initial velocity distribution). The initial rovibrational state (v, j) as well as the orientation of the molecular rotational state specified by the projection quantum number m onto the initial relative velocity vector between the collision partners is prepared by the Stark-induced adiabatic Raman Passage (SARP) method.[17,18] This approach eliminates the requirement of external electromagnetic fields to confine and control molecules during the collision process and enables collisional studies of molecules that are not amenable to external field control. Perreault *et al.* showed that rotational quenching of HD ($v = 1, j = 2$) in collisions with H_2, D_2 and He depends strongly on whether the initial HD molecular bond axis is preferentially aligned horizontal (H-SARP) or vertical (V-SARP) to the initial relative velocity vector. For more details of the intra-beam method for cold and ultracold collisions we refer to recent works of Amarasinghe *et al.*[46,47]

The pioneering experiments of Perreault *et al.* motivated theoretical studies[48–51] that revealed rotational quenching of HD by H_2 and He is governed by isolated shape resonances near a collision energy of $\sim$ 1 K. Thus, stereodynamic control of the resonance features provides a direct handle to influence the collision outcome. As shown in a recent theoretical study, such control is not limited to isolated shape resonances but also in the presence of overlapping shape resonances, as demonstrated for the H_2+HCl[52] system that is characterized by a stronger anisotropic interaction than H_2+HD.

While these successful demonstrations are promising, it implies that stereodynamic control is effective only in the energy

a)Electronic mail: masatomorita2013@gmail.com
b)Electronic mail: naduvala@unlv.nevada.edu

region where one or more shape resonances exist. In other words, it is difficult to control collision outcomes utilizing the m-dependence of cross sections (stereodynamic preference) in the ultracold energy regime (< 1 mK) dominated by an incoming s-wave ($l = 0$ partial wave). Furthermore, it has been shown that stereodynamic control of collisional rotational transition and chemical reaction is not possible at the level of the integral cross section (ICS) for the $l = 0$ partial wave.[53] Nonetheless, here we show that there exists complex stereodynamics in the ultracold energy regime and the control of the outcomes by preparing initial m is still possible by a selective measurement of inelastically scattered molecules in an oriented rotational state designated by m'. We demonstrate that both m and m'-resolved measurements can reveal significant stereodynamic effect over a wide range of energy regardless of the presence of a shape resonance.

In this paper, we examine He+HD collisions as an illustrative case as it has already been studied by the SARP experiment and is a benchmark system for both experiment and theory. Use of He as the collision partner also avoids the difficulty of preparing H_2 in a single rotational level of *ortho* (nuclear spin $I = 1$, odd rotational levels) or *para* (nuclear spin $I = 0$, even rotational levels) states due to thermal population of rotational states.[14,15] Further, highly accurate potential energy surfaces (PESs) with spectroscopic accuracy are available for the HeH_2 system.[54–56] Indeed, our recent study[51] of rotational quenching of HD ($v = 1, j = 2 \rightarrow v' = 1, j = 0$) in cold collisions with He yielded good agreement with experimental results of Perreault *et al.*[16] for the angular distribution of inelastically scattered HD.

The paper is organized as follows: Section II provides a brief outline of the theory and computational details. Results for rotational quenching processes $v = 1, j = 2 \rightarrow v' = 1, j' = 1$ (Section III A) and $v = 1, j = 3 \rightarrow v' = 1, j' = 2$ (Section III B) are presented in Section III and a summary of our findings is given in Section IV.

II. THEORY AND COMPUTATION

A. Scattering formalism

The quantum mechanical scattering problem of collisions between He (^{1}S) and HD ($^1\Sigma$) is numerically solved using the MOLSCAT (v.14) code[57]. It implements solution of the close-coupling (CC) equations[58] derived from the time-independent Schrödinger equation using the total angular momentum representation in the space-fixed (SF) coordinate frame.

The Hamiltonian for the collision complex of He+HD may be written ($\hbar = 1$) in Jacobi coordinate as

$$\hat{\mathscr{H}} = -\frac{1}{2\mu R}\frac{d^2}{dR^2}R + \frac{\hat{l}^2}{2\mu R^2} + \hat{h}_{\rm HD} + V_{\rm int}(R, r, \gamma), \quad (1)$$

where $\mu(= 1.721871434$ amu) is the reduced mass of He and HD, $\hat{l}$ is the orbital angular momentum operator for the relative motion of He and HD, and $\hat{h}_{\rm HD}$ is the rovibrational Hamiltonian for the isolated HD molecule. The interaction potential $V_{\rm int}(R, r, \gamma)$ between He and HD in the electronic ground state is generated from the BSP3 PES for the HeH_2 system.[54]

The total wavefunction for a given value of the total angular momentum J of the collision complex, its projection component M onto the SF z-axis, and the inversion parity $\varepsilon_I = (-1)^{j+l}$ (all three quantities are conserved during the collision) is expanded as

$$\Psi^{JM\varepsilon_I} = \frac{1}{R}\sum_{vjl} F_{vjl}^{JM\varepsilon_I}(R)\frac{\chi_v^j(r)}{r}|JM\varepsilon_I(lj)> \quad (2)$$

where $F_{vjl}^{JM\varepsilon_I}(R)$ are the radial expansion coefficients in R, $\chi_v^j(r)$ denote rovibrational eigenfunctions of HD specified by quantum numbers of v and j, and $|JM\varepsilon_I(lj)>$ denotes basis functions for the angular degrees of freedom in the total angular momentum representation for a given parity ε_I.

The coefficients $F_{vjl}^{JM\varepsilon_I}(R)$ satisfy the CC equations obtained by substituting Eq. (2) into the time-independent Schrödinger equation,

$$\left[\frac{1}{2\mu}\frac{d^2}{dR^2} - \frac{l(l+1)}{2\mu R^2} + E_C\right]F_{vjl}^{J\varepsilon_I}(R) = \sum_{v'j'l'} F_{v'j'l'}^{J\varepsilon_I}(R)\int_0^\infty \langle J\varepsilon_I(lj)|\chi_v^j(r)V_{\rm int}(R,r,\gamma)\chi_{v'}^{j'}(r)|J\varepsilon_I(l'j')\rangle dr, \quad (3)$$

where M is omitted since the CC equations are independent of M. The collision energy E_C is given by $E_C = E - E_{v,j}$ where E denotes the total energy and $E_{v,j}$ denote the rovibrational energies of the HD molecule obtained by solving the eigenvalue problem

$$\left[-\frac{1}{2\mu_{\rm HD}}\frac{d^2}{dr^2} + \frac{j(j+1)}{2\mu_{\rm HD}r^2} + V_{\rm HD}(r)\right]\chi_v^j(r) = E_{v,j}\chi_v^j(r), \quad (4)$$

where $\mu_{\rm HD}(= 0.6716999$ amu) is the reduced mass of HD. For the potential energy curve $V_{\rm HD}(r)$ in the electronic ground state of the HD molecule, we adopt a modified version of Schwenke's H_2 potential ($X^1\Sigma_g^+$) reported by Boothroyd *et al.*[59] The modified log-derivative propagation method of Manolopoulos[60] is employed to numerically solve the CC equations from $R = 2.0$ Å to 50.0 Å with a propagation interval of $\Delta R = 0.05$ Å.

As discussed in our recent work[51] the BSP3 PES[54] used in our calculations is the most accurate *ab initio* PES for the HeH_2 system and it yields line-shape parameters of H_2 and HD immersed in He in excellent (subpercent) agreement with highly accurate experimental results[55,56]. The uncertainty of the BSP3 PES in the van der Walls well region is estimated to be less than 0.04 K, sufficiently below the mean collision energies in the experiments of Perreault *et al.*[16] As illustrated in our previous work,[51] other available He-H_2 PESs[59,61] also yield very similar results as the BSP3 PES.

B. Rotational quenching cross section

Solution of the CC equations yields the scattering S-matrix from which scattering amplitudes for various state-to-state transitions specified by quantum numbers (v,j,m) and (v',j',m') can be constructed. Since the S-matrix is evaluated in the total angular momentum representation in the SF coordinate frame, its elements are specified by the quantum numbers (v,j,l) and (v',j',l'). It is necessary to transform the basis set to obtain the scattering amplitudes specified by (v,j,m). Here, we focus on pure rotational transitions within a vibrational manifold, and omit v and the parity designation ε_l for simplicity. Cross sections for vibrational transitions are 5 to 6 orders of magnitude smaller than pure rotational transitions as in H_2+HD[48] and H_2+HCl[52] collisions.

The scattering amplitude for rotational transition between oriented (m and m'-specified) HD rotational states is given by,[22,51,58,62,63]

$$f_{jm\to j'm'}(\theta,\phi,E) = \sqrt{\pi}(-1)^{j+j'}\sum_{J=0}\sum_{l=|J-j|}^{J+j}\sum_{l'=|J-j'|}^{J+j'} i^{l'-l}(2J+1)\sqrt{2l+1} \times \begin{pmatrix} j & l & J \\ m & 0 & -m \end{pmatrix}\begin{pmatrix} j' & l' & J \\ m' & m-m' & -m \end{pmatrix} T^J_{jl,j'l'}(E)Y_{l'm-m'}(\hat{\boldsymbol{R}}), \quad (5)$$

where θ and ϕ are the scattering polar and azimuthal angles, $T(E)$ is the T-matrix obtained from the S-matrix as $T(E) = 1-S(E)$, and Y denotes a spherical harmonic as a function of $\hat{\boldsymbol{R}} = (\theta,\phi)$.

The corresponding differential cross section (DCS) is given by the square of modulus of the scattering amplitude:

$$\frac{d\sigma_{jm\to j'm'}}{d\Omega} = \frac{|f_{jm\to j'm'}(\theta,\phi,E)|^2}{k_C^2}, \quad (6)$$

where $k_C = \sqrt{2\mu E_C}$ is the magnitude of the wave vector in the incident channel. In the experiment of Perreault *et al.*[51] the ϕ-dependence is not observed and the θ-dependence of the DCS is obtained after averaging over ϕ[51],

$$\frac{d\sigma_{jm\to j'm'}}{d\theta} = 2\pi\sin\theta\frac{|f_{jm\to j'm'}(\theta,E)|^2}{k_C^2}, \quad (7)$$

where $f_{jm\to j'm'}(\theta,E)$ is related to the full scattering amplitude of Eq. (5) by the relation $f_{jm\to j'm'}(\theta,\phi,E) = f_{jm\to j'm'}(\theta,E)\exp\{-i(m-m')\phi\}$. The ICS ($\sigma_{jm\to j'm'}$) is obtained by taking an integral of the DCS over θ from 0 to π.

In our previous studies,[51] we examined the quenching from $v=1, j=2$ to $v'=1, j'=0$ for comparison with experiment results of Perreault *et al.*[16] Here, we consider the stereodynamic effect of the quenching to $v'=1, j'=1$ from the same initial rovibrational state with a focus on the ultracold regime. We show that significant stereodynamic effect can be observed in the ultracold energy regime by selective measurement of the inelastically scattered HD ($v'=1, j'=1$) in an orientation specified by the value of m'. Similar effect is reported for quenching from $v=1, j=3$ to $v'=1, j'=2$.

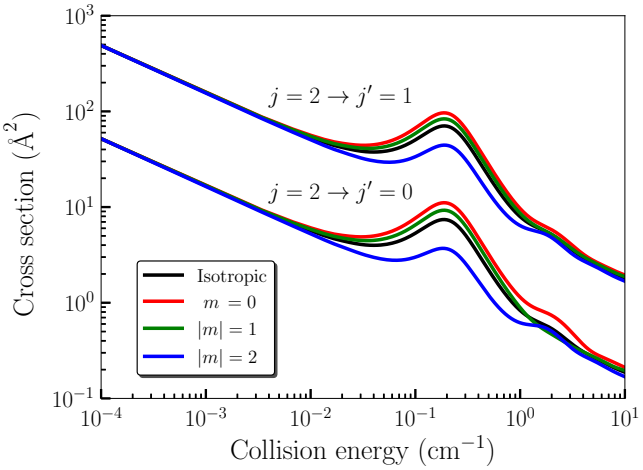

FIG. 1. Integral cross sections for rotational quenching of initially prepared HD ($v=1, j=2, m$) to ($v'=1, j'=0$) and ($v'=1, j'=1$) in collisions with He. Initial m-dependence is displayed with red ($m=0$), green ($|m|=1$), and blue ($|m|=2$). Non polarized case without preparation of m is displayed in black (isotropic).

III. RESULTS AND DISCUSSIONS

A. $v=1, j=2\to v'=1, j'=1$

Figure 1 shows the calculated ICS for the rotational quenching of initially oriented HD ($v=1, j=2, m$) by collisions with He to $j'=0$ ($\Delta j=-2$) and $j'=1$ ($\Delta j=-1$) within the $v=1$ manifold. We note that $|m|$ in the legend of the figure means that the resultant cross section is independent of the sign of m, thus the cross section is invariant even if we prepare the molecule in a state described by a coherent superposition of $|j,-m>$ and $|j,m>$ with any (normalized) expansion coefficients. Effects of relative phases in initial coherent superposition of different m states is not observed unless we observe the DCS with ϕ resolution. The results for $j=2\to j'=0$ are the same as those reported previously.[51] As discussed in our previous paper, the primary peak centered around a collision energy of 0.2 cm^{-1} and the shoulder around 2 cm^{-1} are due to shape resonances from incoming p-wave ($l=1$) and d-wave ($l=2$), respectively. Except for the overall magnitude, the ICSs for both $j'=0$ and $j'=1$ feature similar energy dependence and m-dependence. The higher magnitude for $|\Delta j|=1$ reflects the leading anisotropic term $V_1(R,r)$ in the angular dependence of the interaction potential ($V_{\rm int}(R,r,\gamma) = \sum_\lambda V_\lambda(R,r)P_\lambda(\cos\gamma)$ where P_λ is a Legendre polynomial) that drives the $|\Delta j|=1$ transition. Note that unlike He-H_2, the leading $V_\lambda(R,r)$ terms of odd order in λ are non-zero for He-HD.

The m-dependence in the ICSs is pronounced only around the resonances for both transitions consistent with previous theoretical results for other systems.[49,50,52] Thus, it is expected that the stereodynamic control of collision outcomes by preparing the initial molecular rotational state in an orientation specified by the value of m is most effective in the region of a shape resonance. It has been shown rigorously

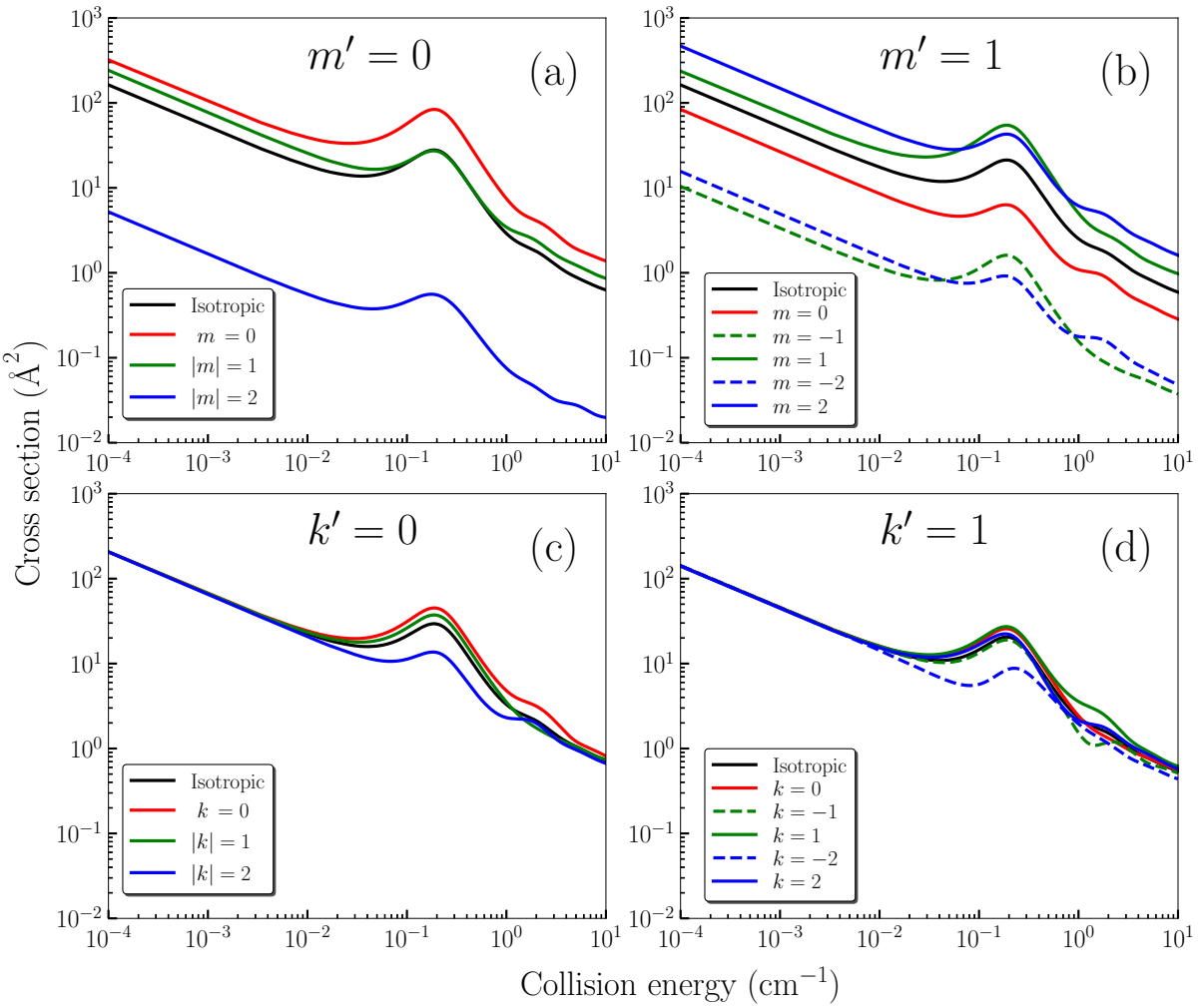

FIG. 2. Integral cross sections for rotational quenching of initially prepared HD ($v = 1, j = 2, m$) to ($v' = 1, j' = 1, m'$) in collisions with He: (a) $m' = 0$; (b) $m' = 1$. Results for $m' = -1$ are identical to (b) by inverting the sign of m in the legend. Results for initial k and final k' helicity dependences are displayed in (c) and (d) for $k' = 0$ and $k' = 1$, respectively. Results for $k' = -1$ are identical to (d) by inverting the sign of k in the legend.

that there is no m-dependence for the ICS in s-wave collisions even if the molecule has internal angular momenta such as spin or electronic orbital angular momentum in addition to the rotational angular momentum.[53] These findings raise the following questions: 1). Is stereodynamics relevant in the ultracold energy regime? and 2). Does the similar qualitative m-dependence of the ICS between $\Delta j = -1$ and $\Delta j = -2$ imply that these processes are driven by similar dynamic effects and are not influenced by stereodynamic preparation?

To address the above questions, for $j = 2 \rightarrow j' = 1$, we decompose the ICS into the 3 contributions designated by the m' values ($m' = -1, 0, 1$ for $j' = 1$) although such m' selective detection has not been realized in the experiments of Perreault *et al*. However, we note that Perreault *et al*.[14] indirectly extracted the m, m' dependence for HD+D_2 collisions by fitting the observed angular distributions of inelastically scattered HD to an of expansion of relevant outgoing partial waves present in the experiment. Recently, Sharples *et al*.[31] reported four vector correlation between relative velocities and rotational angular momenta in initial and final states, namely $\boldsymbol{k}$-$\boldsymbol{j}$-$\boldsymbol{k'}$-$\boldsymbol{j'}$ correlation ($\boldsymbol{k}$: relative momentum), for collisions of electronically excited NO ($A\,^2\Sigma^+$) with Ne by observing the scattering angle dependence of ionization probabilities using a circularly polarized light at a collision energy of about 680 cm^{-1}.

In Fig. 2 (a) and (b), we show the m-dependence of the ICS for $m' = 0$ and $m' = 1$, respectively, for the $j' = 1$ state. In (a), we see a significant m-dependence for the cross section in the entire energy region including the ultracold energy regime dominated by the Wigner threshold behavior. The largest cross section corresponds to $m = 0 \rightarrow m' = 0$ that conserves m. On the other hand, more than an order of magnitude suppression is observed in the quenching from $|m| = 2$. We note that the ICS with any type of initial rotational state preparation, including the HD bond axis alignment performed previously in the SARP experiment, is given as the sum of these cross sections in (a) with positive valued weighting factors,[50,51] thus the upper and lower limits of the control

range with initial HD preparation is given by the red ($m = 0 \rightarrow m' = 0$) and blue ($|m| = 2 \rightarrow m' = 0$) curves, respectively. In Fig. 2 (b), the ICS for $m = 2 \rightarrow m' = 1$ (blue solid curve) is the largest, and the m-conserving process $m = 1 \rightarrow m' = 1$ (green solid curve) becomes largest only in the vicinity of the $l = 1$ resonance (0.2 cm^{-1}) indicating that the stereodynamic preference may largely depend on the partial wave (l) and collision energy. On the other hand, the efficiencies for processes that involve a change in the sign of m (dashed lines, $|\Delta m| = 2$ and 3) are largely suppressed. Including the blue curve in (a) for $|m| = 2$ ($|\Delta m| = 2$), significant suppression of the ICS for these processes in the ultracold energy (s-wave) regime correlates with the restriction on the number of outgoing partial waves. For the initial rotational sate of $j = 2$, the total angular momentum quantum number for the collision complex with the incoming s-wave ($l = 0$) is $J = 2$, thus, due to the conservation of the total angular momentum and the parity ($J = J'$ and $(-1)^{j+l} = (-1)^{j'+l'}$), the possible outgoing partial waves for the final rotational state of $j' = 1$ are $l' = 1$ and 3. Furthermore, due to the conservation of the projection of J, the relation $M = m + m_l = m' + m_{l'}$ is satisfied for the sum of the projections of rotational and orbital angular momenta yielding $m_{l'} = m - m'$ for the case of $l = 0$ ($m_l = 0$), thus the $l' = 1$ component cannot exist for the processes $|\Delta m| \geq 2$. A suppression of ICS with increasing $|\Delta m|$ was also reported by Krems and Dalgarno[27] for the reorientation of electronic angular momentum in O($^3P_{j=2,m=2}$)+He collisions at ultracold temperatures.

The non-polarized cross sections without preparing the initial orientation (black solid curves) show very similar behavior in (a) and (b) and that m' selective measurement without preparing the initial orientation (m) is not useful in gaining insights into the stereodynamics in the ultracold energy regime. In all, the hidden information on stereodynamics in the ultracold energy regime is revealed only when the ICS examined with both m and m' resolution. While the m-dependence for $j = 2 \rightarrow j' = 1$ and $j = 2 \rightarrow j' = 0$ in Fig. 1 is similar when m' is not resolved, stereodynamics of $j = 2 \rightarrow j' = 1$ reveals a much more intricate picture when m' is specified. The quenching to the rotational ground state ($j' = 0$) does not exhibit m-dependence because there is only a single $m' = 0$ component (no m' resolution). We omit the results for $m' = -1$ because they can be obtained by inverting the sign of m in the legend in Fig. 2 (b).

Next, we point out that some qualitative features in stereodynamic preference (order of magnitude of ICS with respect to m and m') are independent of the system in the ultracold energy regime. In Eq. (5), for the incoming s-wave ($l = 0$), there are two possible terms related to the $l' = 1$ and 3 outgoing partial waves for $J = 2$, $j = 2$ and $j' = 1$ as discussed above. For each l', the relative m, m' dependence for the partial ICS is determined by the product of two 3-j symbols since the T-matrix element is independent of m and m', and the integral of the square of the modulus of spherical harmonic $Y_{l',m-m'}$ over θ yields unity in evaluating ICS. As discussed in our previous work,[51] for $m' = 0$ in Fig. 2 (a), the ratio of the partial ICS for $l' = 1$ is $1 : 0.75$ for $m = 0$ and $|1|$ (see Appendix A for more details) and zero for $|m| = 2$. On the other hand, for $l' = 3$, the ratio of the partial ICS with $m' = 0$ is $1 : 0.89 : 0.56$ for $m = 0$, $|1|$ and $|2|$, respectively. Thus, we can conclude that for $m' = 0$ the stereodynamic preference is $m = 0 > |m| = 1 > |m| = 2$ regardless of the value of the T-matrix elements which are system dependent. This trend is clearly displayed in Fig. 2 (a). It is important to emphasize that the above trend for the stereodynamic preference comes from purely algebraic character of the scattering amplitude.

An important goal of stereodynamics is to gain insights into how the anisotropy of the interaction potential (interaction force) controls the collision outcome. However, in the s-wave regime, the overall trend in stereodynamic preference may not reflect details of the interaction potential. In such cases, system dependent information coded in the T-matrix (S-matrix) elements is revealed only by quantitative measurements of m, m'- resolved ICS. On the other hand, in the case of $m' = 1$ (Fig. 2 (b)), we cannot predict even qualitative trend of ICS with respect to m without the information of T-matrix since the 3-j symbols give rise to a different trend of stereodynamic preference between $l' = 1$ and $l' = 3$ (see Appendix A). These aspects underscore the difficulty in pinpointing specific stereodynamic preference in the ultracold regime. Yet, it is worth emphasizing that some qualitative trends in stereodynamic preference are independent of the interaction potential for purely s-wave collisions. At higher energies (> 1 cm^{-1}), due to contributions from multiple partial wave, it is difficult to analytically discuss the feature of m, m' dependence. However, the large m-dependence even around 10 cm^{-1} implies that higher partial waves result in mechanisms similar to that of s-wave.

The orientations (m, m') of the initial and final HD rotational states are specified in the SF coordinate frame whose z-axis is parallel to the initial relative velocity for the collision. In the SARP experiments, due to the co-expansion of colliding species, the initial relative velocity is also parallel to the laboratory fixed molecular beam as well as the direction of time-of-flight axis, simplifying the relation between experimental data and scattering properties defined in the SF frame.[14,15] However, to investgate more details of the dynamics as well as hidden propensity rules, it would be worth exploring stereodynamics in other frames. Here, we consider initial and final helicity[64,65] dependence of the ICS in Fig. 2 (c) and (d). The initial projection (helicity) component k is obtained by taking the projection of the molecular rotational angular momentum onto the axis parallel to the incident relative momentum. On the other hand, the final helicity (k') for the inelastically scattered HD (here, $v' = 1, j' = 1$) is defined by the projection onto the direction of the final (recoil) relative momentum. The scattering amplitude in the helicity frame is expressed using the scattering amplitued in SF (Eq. (5)) and the Wigner D-matrix as[22,25]

$$f_{jk(=m)\rightarrow j'k'}(\theta,\phi,E) = \sum_{m'=-j'}^{j'} D^{j'*}_{m'k'}(\phi,\theta,0) f_{jm\rightarrow j'm'}(\theta,\phi,E), \tag{8}$$

where k is equal to m since the quantization z-axis for the initial helicity component is parallel to the initial relative velocity vector. Similar to the transformation between SF

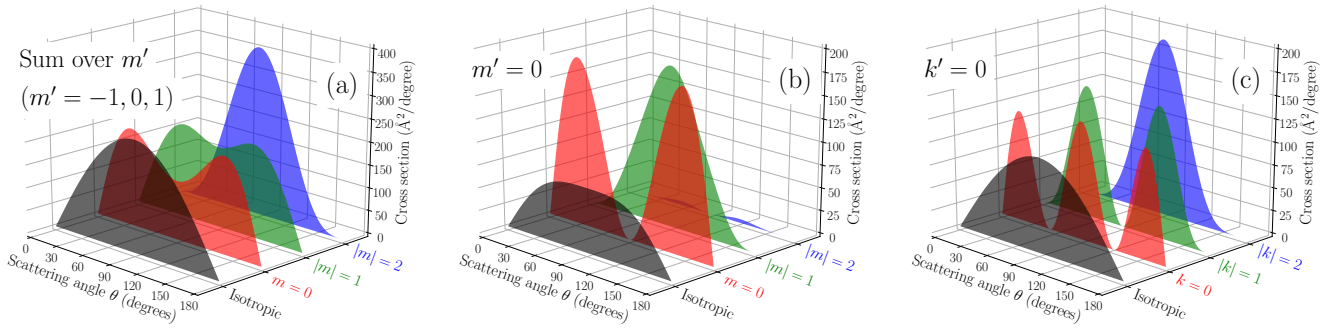

FIG. 3. Differential cross sections for rotational quenching of initially prepared HD ($v = 1, j = 2, m$) to ($v' = 1, j' = 1, m'$) in collisions with He at a collision energy of 10^{-4} cm^{-1}. (a) Initial orientation (m) dependence; (b) Initial orientation (m) dependence with $m' = 0$; (c) initial orientation (k) dependence with $k' = 0$ in the helicity frame.

frame and body-fixed (BF) frame, the 3rd Euler angle in the D-matrix is not unique unless we define it. Here, we set the angle to be zero adopting the convention of Alexander.[22] An explicit form of the θ-dependent scattering amplitude similar to $f_{jm\to j'm'}(\theta, E)$ in Eq. (7) is convenient in the following discussion:[65,66]

$$f_{jk\to j'k'}(\theta, E) = \frac{(-1)^{j+j'}}{2} \sum_{J=0} (2J+1) d^J_{k',k}(\theta) \sum_{l=|J-j|}^{J+j} \sum_{l'=|J-j'|}^{J+j'} i^{l'-l+1} \times \sqrt{2l+1}\sqrt{2l'+1} \begin{pmatrix} j & J & l \\ k & -k & 0 \end{pmatrix} \begin{pmatrix} j' & J & l' \\ k' & -k' & 0 \end{pmatrix} T^J_{jl,j'l'}(E). \quad (9)$$

We note that the T-matrix in the right hand side is specified by (j, l) index.

Since k and m are the same, the k-dependence of the ICSs is identical to the m-dependence in Fig. 1 as long as we sum over contributions from all k' ($= -1, 0, 1$) components. On the other hand, once we specify k', the k-dependence (Fig. 2 (c) and (d)) is drastically different from the m-dependence in (a) and (b). Evidently, the k-dependence is significant only around the resonance regions as seen in (c) and (d). Furthermore, the k dependence fades with decreasing the collision energy and it vanishes in the ultracold limit. This particular k independence of the ICS is due to the dominance of s-wave ($l = 0$) and resultant dominance of $J = j$ component. For $J = j$ and $l = 0$, the first 3-j symbol in the right hand side of Eq. (9) results in $(-1)^{J-k}/\sqrt{2J+1} (= (-1)^{j-k}/\sqrt{2j+1})$,[67,68] thus k appears only as a phase factor. The remaining k dependence is captured in the Wigner small d-matrix $d^J_{k',k}(\theta)$. While the behavior of the d-matrix is reflected in the DCS, it has no effect on the magnitude of the ICS once integrated over θ from 0 to π. Thus, as a universal feature, there is no k-dependence in the ICS in the ultracold energy regime even with k'-resolution. This feature applies regardless of the collision energy for the $l = 0$ partial wave. On the other hand, the absolute value of the (k-independent) ICS is system dependent and determined by the T-matrix elements associated with $l' = 1$ and 3.

So far, we have focused on the m/k-dependence in a selected m'/k' component. Now, we shall discuss the final m'/k' distribution with an initial preparation specified by the value of m/k. To obtain the m' distribution, we need to compare the curves with same color in (a) and (b). At the collision energy of 10^{-4} cm^{-1}, the $m' = 0$ to $m' = 1$ ratio of the ICSs (branching ratio) is 3.81, 23.2, 1.02, 0.333, and 0.0113 with initial orientations $m = 0, -1, 1, -2$ and 2, respectively. Here we clearly observe the m-dependence in ICS (Fig. 2 (a) and (b)) and predict branching ratios by resolving final orientation m'. In the same way, we consider the final k' distributions given by the $k' = 0$ to $k' = 1$ ratio of the ICSs at 10^{-4} cm^{-1}. As we can expect from Fig. 2 (c) and (d), the ratio is independent of the initial k value, yielding 1.46 with all possible k values ($k = 0, -1, 1, -2$ and 2), implying that the branching ratio is similar to a statistical (uniform) distribution. We note that the branching ratio is not universal because it determined by the T-matrix elements associated with $l' = 1$ and 3.

We described the same stereodynamics in two different frames (SF vs helicity), thus the different final distributions of the (projection) components are not necessarily important. Previous studies of the m, m'-dependence at higher collision energies ($\sim$ 10 cm^{-1} to $\sim$ 1000 cm^{-1}) have addressed frame dependence to explore the Δm propensity and develop associated approximation methods.[22,25,26,28,30] Indeed, a statistical distribution[22,25] as well as asymmetric distribution with respect to the sign of m'/k' were observed in some cases. However, to our knowledge, a significant m'-dependence similar to the one presented here was not reported. Previous studies analyzed the frame dependence based on the difference in the interaction potentials in the short-range repulsive and long-rang attractive regions, and the resultant scattering directions. It is not obvious whether such criterion is effective also in the ultracold energy regime where both the long-range and short-range forces strongly influence the scattering dynamics and the collision is dominated by a single incoming partial wave. Furthermore, as pointed above, the qualitative orientation dependence in the cross section is not necessarily related to the system dependent properties such as interaction potential energy surface. There might

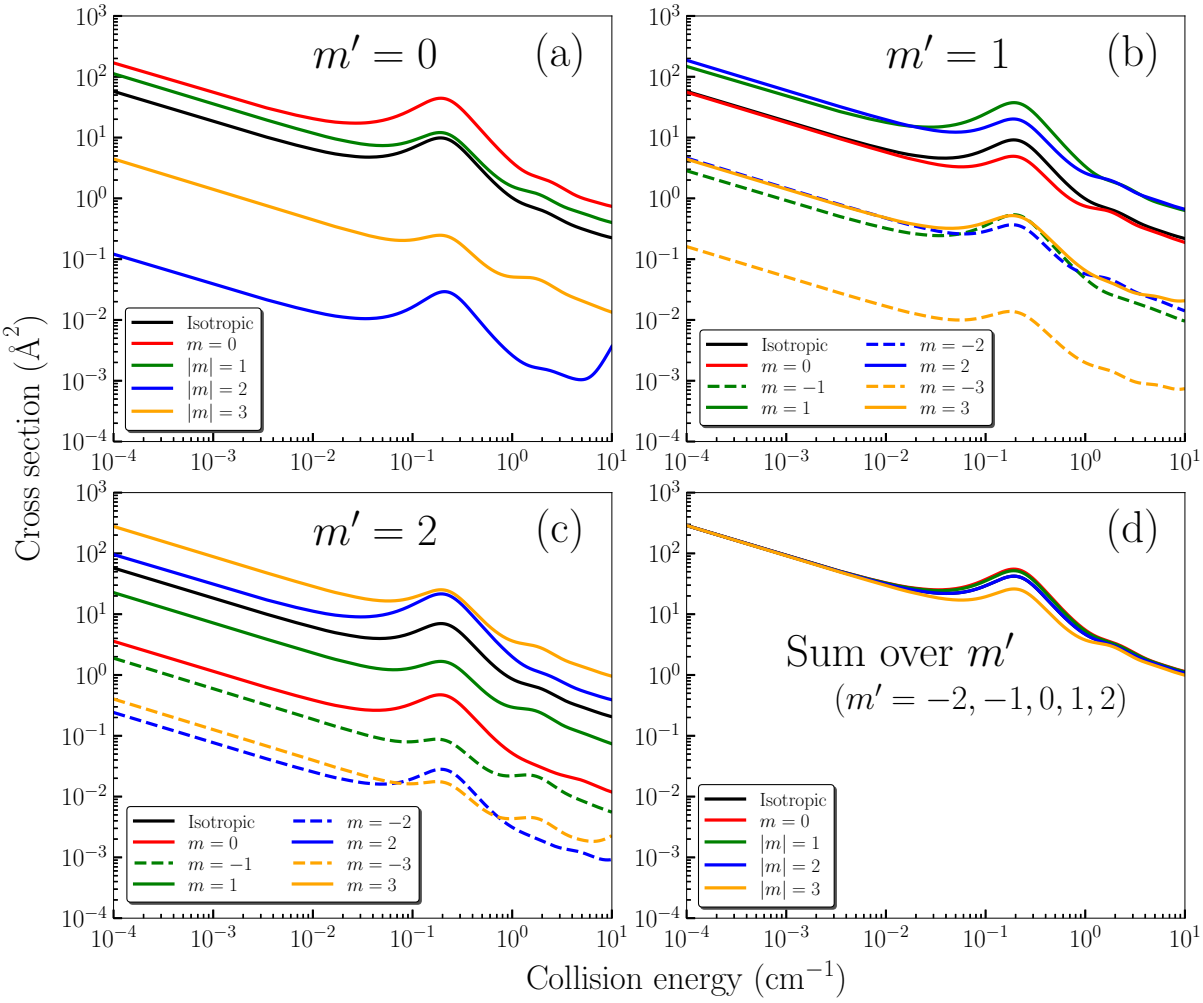

FIG. 4. Integral cross sections for rotational quenching of initially prepared HD ($v = 1, j = 3, m$) to ($v' = 1, j' = 2, m'$) in collisions with He: (a) $m' = 0$; (b) $m' = 1$. Results for $m' = -1$ are identical to (b) by inverting the sign of m in the legend. Results for initial k and final k' helicity dependences are displayed in (c) and (d) for $k' = 0$ and $k' = 1$, respectively. Results for $k' = -1$ are identical to (d) by inverting the sign of k in the legend.

exist a frame exhibiting a specific propensity rule in ultracold collisions but an elaborate systematic search for finding such a frame is beyond the scope of this work.

Next, we examine the effect of m'/k' selection on the m/k-dependence for the differential cross section (DCS). Such fully resolved DCS corresponds to $\boldsymbol{k}$-$\boldsymbol{j}$-$\boldsymbol{k}'$-$\boldsymbol{j}'$ correlation and has recently been reported for collisions of NO with rare-gas atoms at around 500 to 700 cm^{-1} to analyze irregular diffraction patterns for NO and identify propensity rules.[30] Unlike ICS, DCS can exhibit m-dependence even at ultracold energies without m' resolution.[53] However, as shown in Fig. 3 (a), the m-dependence for the DCS is actually very weak at a collision energy of 10^{-4} cm^{-1} if we sum over all m'. We note that the m-dependence in (a) is equal to k-dependence as long as we sum over all k' components since m is equal to k as discussed above. With non-polarized initial HD (black), the DCS is characterized by the $\sin\theta$ in Eq. (7) indicating the isotropic character of the DCS in the form of Eq. (6) for s-wave as discussed by Aldegunde *et al.*[53] Thus, without m' resolution it is very difficult to detect the m-dependence of the DCS in the ultracold energy regime. On the other hand, the m'-resolved DCS ((b) $m' = 0$) exhibits a large m-dependence both in the magnitude and oscillatory behavior (θ-dependence). Compared to (a), it is easy to observe the m-dependence even without fine resolution in θ and absolute magnitude. The results in the helicity frame in (c) exhibit distinct oscillations in θ for different k, thus k' resolution has a substantial impact on the DCS in the ultracold energy regime in the helicity frame unlike ICS (Fig. 2 (c) and (d)). In other words, the integrals of the DCSs in Fig. 3 (c) over θ result in essentially identical ICS values regardless of the value k.

B. $v = 1, j = 3 \rightarrow v' = 1, j' = 2$

Finally, in Fig. 4, we present the ICS for the rotational quenching of initially oriented HD ($v = 1, j = 3, m$) by collisions with He to $j' = 2$ within the $v = 1$ manifold. Similar to

the $j = 2$ results in Fig. 1, the ICS exhibits a primary peak due to the $l = 1$ shape resonance near 0.2 cm^{-1} and a shoulder due to the $l = 2$ partial wave in the 1-3 cm^{-1} regime. We observe strong m-dependence of the ICS with m' resolution as shown in Fig. 4 (a) to (c). Compared to Fig. 2 (a) and (b), the basic trend in m-dependence prevails except for the number of possible values of m. Again, Δm transitions that involve a sign change of m are significantly suppressed. The quenching rate generally decreases with increase in $|\Delta m|$ with some exceptions. For example, the $|\Delta m|$ propensity is reversed between $|m| = 2 \rightarrow m' = 0$ and $|m| = 3 \rightarrow m' = 0$ in (a). We see that the order of magnitude of the control range of the ICS with respect to m is larger than that in Fig. 2 (a) and (b) for $j = 2$. Thus, it may be possible to expand the range of control for higher initial rotational states. The panel (d) in Fig. 4 shows results obtained by adding the contributions from all possible $m'(= -2, -1, 0, 1, 2)$ (similar to Fig. 1) indicating that the conventional stereodynamic control of the collision outcomes is not effective except in the resonance region.

The m' distribution for a given m at a collision energy of 10^{-4} cm^{-1} is as follows: the $m' = 0$ to $m' = 1$ ratio of the ICSs is 3.03, 39.5, 0.759, 0.026, 0.0006, 27.7, 1.01 for $m = 0, -1, 1, -2, 2, -3$ and 3, respectively and the $m' = 0$ to $m' = 2$ ratio is 47.1, 59.3, 4.95, 0.50, 0.0013, 11.1, 0.016 for $m = 0, -1, 1, -2, 2, -3$ and 3, respectively. Again, this leads to a highly asymmetric final distribution with respect to the sign and magnitude of m'. We omit the corresponding results in the helicity frame as the k-dependence is limited to the resonance regions even with k' resolution as in Fig. 2 (c) and (d).

IV. SUMMARY AND CONCLUSIONS

We have carried out rigorous quantum scattering calculations of m and m' resolved cross sections in He+HD ($v = 1,\ j,\ m$) $\rightarrow$ He+HD ($v' = 1,\ j',\ m'$) collisions for the $j = 2$ to $j' = 1$ and $j = 3$ to $j' = 2$ transitions in an energy range of 10^{-4} to 10 cm^{-1} spanning the ultracold and cold regimes. For both transitions, the integral cross sections display a $l = 1$ shape resonance near 0.2 cm^{-1} and a shoulder feature from a $l = 2$ partial wave in the 1-3 cm^{-1} regime similar to the previously studied $j = 2$ to $j' = 0$ transition.

Key findings of this work are summarized below:

- For a given initial rotational level, the stereodynamic preference for the different final rotational levels is found to be similar even in the resonance region if the orientation of the final rotational state is not specified by resolving the m' quantum number. However, this result is not universal and may depend on the molecular system.

- There exists intricate stereodynamics in the ultracold regime that is revealed only by resolving the cross sections in both m and m'.

- No initial helicity ($k(= m)$)-dependence for the integral cross section even by detecting inelastically scattered HD in a given helicity (k') component.

- Stereodynamic preference is frame-dependent in the ultracold regime. However, this vanishes for the integral cross section when summed over all possible m'/k' components.

- The m-dependence of each m' component of ICS is partly accounted for without details of the T-matrix elements (and in turn, the details of the interaction potential). Similar universal trend has been discussed in our previous study[51] in the region of a $l = 1$ partial wave shape resonance.

Our findings indicate that stereodynamic control of collision outcomes in the ultracold energy regime governed by the $l = 0$ partial wave is possible if selective measurements of the orientation of final rotational states are carried out. As discussed before m'-dependence of the differential cross section for rotationally inelastic collisions of HD by D_2 has been extracted in the experiment of Perreault *et al.*[14] through a partial wave analysis and a non-linear fit to experimental data. However, their analysis includes $l = 0$ and a few higher-order partial waves and explicit nature of the stereodynamics for the purely s-wave regime was not revealed. It is our expectation that sensitive detection schemes may allow direct m'-resolved measurements and even attain the $l = 0$ regime for collisions involving light species with similar masses (e.g., intrabeam collisions of ^{3}He and HD) or merged beam techniques.

The analysis of the scattering amplitudes in the helicity frame and the k, k' dependence of the resultant integral cross section may provide additional insights into the dynamics and sensitive comparisons between theory and experiment. Our findings indicate that the m, m' analyses similar to those performed in earlier studies for discussing the propensities in various frames may also be effective in the ultracold energy regime.

The results presented here are for collisions in the absence of external fields and motivated by the SARP experiments which use co-expansion of colliding species in a co-propagating molecular beam. It may also apply to buffer-gas cooled molecules or merged beam techniques which are applicable to a broader class of molecules. Many techniques for cooling, trapping, and controlling cold molecule collisions involve external electric and/or magnetic fields and open shell molecules. The degeneracy of the rotational levels will be lifted in an external field and this would affect preparation of initial state, especially when a linear combination of initial m-states are involved as in the case of V-SARP. Also, for collisions in confined geometries, stereodynamics may play an even greater role in ultracold collisions[39,69].

DEDICATION

This paper is dedicated to Kate Kirby for her outstanding contributions in Chemical Physics and AMO Physics as well as her leadership role in serving the physics community.

ACKNOWLEDGMENTS

This work is supported in part by NSF grant No. PHY-1806334 (N.B.) and ARO MURI grant No. W911NF-19-1-0283 (N.B.). We thank Nandini Mukherjee for helpful discussions.

DATA AVAILABILITY STATEMENT

The data that support the findings of this study are available within the article.

Appendix A

As discussed in the main text, the product of two 3-j symbols in the term associated with the incoming s-wave ($l = 0$) and an outgoing partial wave l' in the scattering amplitude (Eq. (5)) determines the relative m, m' dependence of the partial ICS in the ultracold energy regime. Since the cross section is related to the square of the modulus of the scattering amplitude, the key quantity is

$$\left|\begin{pmatrix} j & l & J \\ m & 0 & -m \end{pmatrix}\begin{pmatrix} j' & l' & J \\ m' & m-m' & -m \end{pmatrix}\right|^2. \tag{A1}$$

For the quenching of HD ($j = 2, m \to j' = 1, m'$) in the s-wave regime outgoing partial waves $l' = 1$ and 3 contribute. For $l' = 1$, the m-dependence of the ICS for $m' = 0$ (Fig. 2 (a)) is determined by

$$\left|\begin{pmatrix} 2 & 0 & 2 \\ m & 0 & -m \end{pmatrix}\begin{pmatrix} 1 & 1 & 2 \\ 0 & m & -m \end{pmatrix}\right|^2. \tag{A2}$$

Evaluating the 3-j symbols yields[67,68], for the ratio of the ICS, $1 : 0.75$ for $m = 0$ and $|1|$ and zero for $|m| = 2$ as discussed in the main text. We note that the first 3-j symbol results in $(-1)^{-m}/\sqrt{5}$ in which the m value determines only the sign, thus the second 3-j symbol controls the ratio of the ICS with respect to m. For the $l' = 3$ term,

$$\left|\begin{pmatrix} 2 & 0 & 2 \\ m & 0 & -m \end{pmatrix}\begin{pmatrix} 1 & 3 & 2 \\ 0 & m & -m \end{pmatrix}\right|^2, \tag{A3}$$

the ratio is $1 : 0.89 : 0.56$ for $m = 0$, $|1|$ and $|2|$ for the ICS. From these results, we can conclude that the ratio of the ICS in the ultracold energy regime is $m = 0 > |m| = 1 > |m| = 2$ for $m' = 0$ as shown in Fig. 2 (a). On the other hand, the relative contribution between $l' = 1$ and 3 is system and energy dependent because it is determined by the values of the respective T-matrix elements in Eq. (5). Thus the ratio of the total (sum of the $l' = 1$ and 3 contributions) ICSs with respect to m in Fig. 2 (a) reflects the system dependent information such as the interaction potential.

For $m' = 1$ (Fig. 2 (b)), we can perform similar analysis for $l' = 1$ and $l' = 3$. However, as shown below, the resultant relative ratios for the partial ICS with respect to m show a different trend between $l' = 1$ and $l' = 3$. Thus, for an accurate prediction of the trend in the magnitude of total ICS the T-matrix information also needs to be considered. For the $l' = 1$ component,

$$\left|\begin{pmatrix} 2 & 0 & 2 \\ m & 0 & -m \end{pmatrix}\begin{pmatrix} 1 & 1 & 2 \\ 1 & m-1 & -m \end{pmatrix}\right|^2 \tag{A4}$$

yields the ratio of the partial ICS to be $0.17 : 0.5 : 1$ for $m = 0, 1$ and 2, respectively. Here, $m = -1$ and -2 result in 0 as discussed in the main text. For the $l' = 3$ component,

$$\left|\begin{pmatrix} 2 & 0 & 2 \\ m & 0 & -m \end{pmatrix}\begin{pmatrix} 1 & 3 & 2 \\ 1 & m-1 & -m \end{pmatrix}\right|^2 \tag{A5}$$

yields $1 : 0.5 : 0.17 : 1.7 : 2.5$ for $m = 0$, 1, 2, -1 and -2 for the ICS ratio, thus $m = -2$ shows the largest partial ICS. The ratio of Eq. (A4) with $m = 2$ ($l' = 1$) to Eq. (A5) with $m = -2$ ($l' = 3$) is 1.4. Therefore, to explain the significant difference of $m = 2$ and $m = -2$ in Fig. 2 (b), the square of the modulus of the T-matrix element associated with $l' = 1$ is much larger than that with $l' = 3$ (In fact, the actual ratio of the square of the modulus of the T-matrix elements of $l' = 1$ and $l' = 3$ is 21.3 at 10^{-4} cm^{-1}).

[1] K. M. Jones, E. Tiesinga, P. D. Lett, and P. S. Julienne, "Ultracold photoassociation spectroscopy: Long-range molecules and atomic scattering," Rev. Mod. Phys. **78**, 483–535 (2006).

[2] R. V. Krems, "Cold controlled chemistry," Phys. Chem. Chem. Phys. **10**, 4079–4092 (2008).

[3] L. D. Carr, D. DeMille, R. V. Krems, and J. Ye, "Cold and ultracold molecules: science, technology and applications," New J. Phys. **11**, 055049 (2009).

[4] C. Naulin and M. Costes, "Experimental search for scattering resonances in near cold molecular collisions," Int. Rev. Phys. Chem. **33**, 427–446 (2014).

[5] B. K. Stuhl, M. T. Hummon, and J. Ye, "Cold state-selected molecular collisions and reactions," Annu. Rev. Phys. Chem. **65**, 501–518 (2014).

[6] N. Balakrishnan, "Perspective: Ultracold molecules and the dawn of cold controlled chemistry," J. Chem. Phys. **145**, 150901 (2016).

[7] J. L. Bohn, A. M. Rey, and J. Ye, "Cold molecules: Progress in quantum engineering of chemistry and quantum matter," Science **357**, 1002–1010 (2017).

[8] M. S. Safronova, D. Budker, D. DeMille, D. F. J. Kimball, A. Derevianko, and C. W. Clark, "Search for new physics with atoms and molecules," Rev. Mod. Phys. **90**, 025008 (2018).

[9] T. Karman and J. M. Hutson, "Microwave shielding of ultracold polar molecules," Phys. Rev. Lett. **121**, 163401 (2018).

[10] L. Lassablière and G. Quéméner, "Controlling the scattering length of ultracold dipolar molecules," Phys. Rev. Lett. **121**, 163402 (2018).

[11] J. Toscano, H. J. Lewandowski, and B. R. Heazlewood, "Cold and controlled chemical reaction dynamics," Phys. Chem. Chem. Phys. **22**, 9180–9194 (2020).

[12] M.-G. Hu, Y. Liu, D. D. Grimes, Y.-W. Lin, A. H. Gheorghe, R. Vexiau, N. Bouloufa-Maafa, O. Dulieu, T. Rosenband, and K.-K. Ni, "Direct observation of bimolecular reactions of ultracold krb molecules," Science **366**, 1111–1115 (2019).

[13] Y. Liu, M.-G. Hu, M. A. Nichols, D. D. Grimes, T. Karman, H. Guo, and K.-K. Ni, "Photo-excitation of long-lived transient intermediates in ultracold reactions," Nat. Phys. (2020).

[14] W. E. Perreault, N. Mukherjee, and R. N. Zare, "Quantum control of molecular collisions at 1 kelvin," Science **358**, 356–359 (2017).

[15] W. E. Perreault, N. Mukherjee, and R. N. Zare, "Cold quantum-controlled rotationally inelastic scattering of HD with H_2 and D_2 reveals collisional partner reorientation," Nat. Chem. **10**, 561–567 (2018).

[16] W. E. Perreault, N. Mukherjee, and R. N. Zare, "HD ($v = 1$, $j = 2$, m) orientation controls HD-He rotationally inelastic scattering near 1 K," J. Chem. Phys. **150**, 174301 (2019).

[17] W. Dong, N. Mukherjee, and R. N. Zare, "Optical preparation of H_2 rovibrational levels with almost complete population transfer," J. Chem. Phys. **139**, 074204 (2013).

[18] N. Mukherjee, W. Dong, and R. N. Zare, "Coherent superposition of M-states in a single rovibrational level of H_2 by stark-induced adiabatic raman passage," J. Chem. Phys. **140**, 074201 (2014).

[19] J. P. Toennies, "The calculation and measurement of cross sections for rotational and vibrational excitation," Annu. Rev. Phys. Chem. **27**, 225–260 (1976).

[20] H. Katô, R. Clark, and A. McCaffery, "Rotational assignments in excited iodine and reorientation by elastic and inelastic collisions from circularly polarized emission," Mol. Phys. **31**, 943–956 (1976).

[21] L. Monchick, "State selected He–HCl collision cross sections," J. Chem. Phys. **67**, 4626–4631 (1977).

[22] M. H. Alexander, "Close-coupling studies of the orientation dependence of rotationally inelastic collisions," J. Chem. Phys. **67**, 2703–2712 (1977).

[23] V. Khare, D. J. Kouri, and R. T. Pack, "On magnetic transitions and the interpretation of the partial wave parameter in the CS and IOS approximations in molecular scattering theory," J. Chem. Phys. **69**, 4419–4430 (1978).

[24] D. Fitz, "On the choice of partial wave parameter for IOS calculations of m-dependent rotationally inelastic cross sections," Chem. Phys. Letts. **55**, 202 – 205 (1978).

[25] V. Khare, D. J. Kouri, and D. K. Hoffman, "Propensity for preserving polarization in rotationally inelastic molecular collisions," J. Chem. Phys. **74**, 2656–2657 (1981).

[26] D. Davies, "Close-coupling calculations of polarized rotational cross sections for (Ar, LiF)," Mol. Phys. **50**, 229–241 (1983).

[27] R. V. Krems and A. Dalgarno, "Threshold laws for collisional reorientation of electronic angular momentum," Phys. Rev. A **67**, 050704 (2003).

[28] T. Orlikowski, "Propensities for preserving polarization in rotationally inelastic He-O_2 collisions," Mol. Phys. **59**, 1215–1225 (1986).

[29] X. Zhang, C. J. Eyles, C. A. Taatjes, D. Ding, and S. Stolte, "A general scaling rule for the collision energy dependence of a rotationally inelastic differential cross-section and its application to NO(X) + He," Phys. Chem. Chem. Phys. **15**, 5620–5635 (2013).

[30] J. Onvlee, S. D. S. Gordon, S. N. Vogels, T. Auth, T. Karman, B. Nichols, A. van der Avoird, G. C. Groenenboom, M. Brouard, and S. Y. T. van de Meerakker, "Imaging quantum stereodynamics through fraunhofer scattering of NO radicals with rare-gas atoms," Nat. Chem. **9**, 226–233 (2017).

[31] T. R. Sharples, J. G. Leng, T. F. M. Luxford, K. G. McKendrick, P. G. Jambrina, F. J. Aoiz, D. W. Chandler, and M. L. Costen, "Non-intuitive rotational reorientation in collisions of NO(A $^2\Sigma^+$) with Ne from direct measurement of a four-vector correlation," Nat. Chem. **10**, 1148–1153 (2018).

[32] R. J. Beuhler, R. B. Bernstein, and K. H. Kramer, "Observation of the reactive asymmetry of methyl iodide. crossed beam study of the reaction of rubidium with oriented methyl iodide molecules," J. Am. Chem. Soc. **88**, 5331–5332 (1966).

[33] D. H. Parker and R. B. Bernstein, "Oriented molecule beams via the electrostatic hexapole: Preparation, characterization, and reactive scattering," Annu. Rev. Phys. Chem. **40**, 561–595 (1989).

[34] P. R. Brooks, "Reactions of oriented molecules," Science **193**, 11–16 (1976).

[35] A. J. Orr-Ewing, "Dynamical stereochemistry of bimolecular reactions," J. Chem. Soc., Faraday Trans. **92**, 881–900 (1996).

[36] M. P. de Miranda and D. C. Clary, "Quantum dynamical stereochemistry of atom-diatom reactions," J. Chem. Phys. **106**, 4509–4521 (1997).

[37] R. N. Zare, "Laser control of chemical reactions," Science **279**, 1875–1879 (1998).

[38] J. Aldegunde, M. P. de Miranda, J. M. Haigh, B. K. Kendrick, V. Sáez-Rábanos, and F. J. Aoiz, "How reactants polarization can be used to change and unravel chemical reactivity," J. Phys. Chem. A **109**, 6200–6217 (2005).

[39] M. H. G. de Miranda, A. Chotia, B. Neyenhuis, D. Wang, G. Quéméner, S. Ospelkaus, J. L. Bohn, J. Ye, and D. S. Jin, "Controlling the quantum stereodynamics of ultracold bimolecular reactions," Nature Physics **7**, 502–507 (2011).

[40] F. Wang, K. Liu, and T. P. Rakitzis, "Revealing the stereospecific chemistry of the reaction of Cl with aligned CHD_3 ($v_1 = 1$)," Nat. Chem. **4**, 636–641 (2012).

[41] B. Nichols, H. Chadwick, S. D. S. Gordon, C. J. Eyles, B. Hornung, M. Brouard, M. H. Alexander, F. J. Aoiz, A. Gijsbertsen, and S. Stolte, "Steric effects and quantum interference in the inelastic scattering of NO(X) + Ar," Chem. Sci. **6**, 2202–2210 (2015).

[42] L. Song, G. C. Groenenboom, A. van der Avoird, C. K. Bishwakarma, G. Sarma, D. H. Parker, and A. G. Suits, "Inelastic scattering of CO with He: Polarization dependent differential state-to-state cross sections," J. Phys. Chem. A **119**, 12526–12537 (2015).

[43] F. J. Aoiz, M. Brouard, S. D. S. Gordon, B. Nichols, S. Stolte, and V. Walpole, "A new perspective: imaging the stereochemistry of molecular collisions," Phys. Chem. Chem. Phys. **17**, 30210–30228 (2015).

[44] P. G. Jambrina, M. Menéndez, A. Zanchet, E. García, and F. J. Aoiz, "How reactant polarization can be used to change the effect of interference on reactive collisions," Phys. Chem. Chem. Phys. **21**, 14012–14022 (2019).

[45] R. V. Krems, *Molecules in Electromagnetic Fields* (John Wiley & Sons, Ltd, 2018).

[46] C. Amarasinghe and A. G. Suits, "Intrabeam scattering for ultracold collisions," J. Phys. Chem. Lett. **8**, 5153–5159 (2017).

[47] C. Amarasinghe, C. A. Perera, and A. G. Suits, "A versatile molecular beam apparatus for cold/ultracold collisions," J. Chem. Phys. **152**, 184201 (2020).

[48] J. F. E. Croft, N. Balakrishnan, M. Huang, and H. Guo, "Unraveling the stereodynamics of cold controlled HD-H_2 collisions," Phys. Rev. Lett. **121**, 113401 (2018).

[49] P. G. Jambrina, J. F. E. Croft, H. Guo, M. Brouard, N. Balakrishnan, and F. J. Aoiz, "Stereodynamical control of a quantum scattering resonance in cold molecular collisions," Phys. Rev. Lett. **123**, 043401 (2019).

[50] J. F. E. Croft and N. Balakrishnan, "Controlling rotational quenching rates in cold molecular collisions," J. Chem. Phys. **150**, 164302 (2019).

[51] M. Morita and N. Balakrishnan, "Stereodynamics of rotationally inelastic scattering in cold He+HD collisions," J. Chem. Phys. **153**, 091101 (2020).

[52] M. Morita, Q. Yao, C. Xie, H. Guo, and N. Balakrishnan, "Stereodynamic control of overlapping resonances in cold molecular collisions," Phys. Rev. Research **2**, 032018 (2020).

[53] J. Aldegunde, J. M. Alvariño, M. P. de Miranda, V. Sáez Rábanos, and F. J. Aoiz, "Mechanism and control of the F+H_2 reaction at low and ultralow collision energies," J. Chem. Phys. **125**, 133104 (2006).

[54] F. Thibault, K. Patkowski, P. S. Żuchowski, H. Jóźwiak, R. Ciuryło, and P. Wcisło, "Rovibrational line-shape parameters for H_2 in He and new H_2-He potential energy surface," J. Quant. Spectrosc. Radiat. Transf. **202**, 308 – 320 (2017).

[55] M. Słowiński, F. Thibault, Y. Tan, J. Wang, A.-W. Liu, S.-M. Hu, S. Kassi, A. Campargue, M. Konefał, H. Jóźwiak, K. Patkowski, P. Żuchowski, R. Ciuryło, D. Lisak, and P. Wcisło, "H_2-He collisions: Ab initio theory meets cavity-enhanced spectra," Phys. Rev. A **101**, 052705 (2020).

[56] F. Thibault, R. Z. Martínez, D. Bermejo, and P. Wcisło, "Line-shape parameters for the first rotational lines of HD in He," Mol. Astrophys. **19**, 100063 (2020).

[57] J. M. Hutson and S. Green, *MOLSCAT v.14*, Swindon: Engineering and Physical Sciences Research Council (1994).

[58] A. M. Arthurs and A. Dalgarno, "The theory of scattering by a rigid rotator," Proc. R. Soc. London A **256**, 540–551 (1960).

[59] A. I. Boothroyd, P. G. Martin, and M. R. Peterson, "Accurate analytic He-H_2 potential energy surface from a greatly expanded set of ab initio energies," J. Chem. Phys. **119**, 3187–3207 (2003).

[60] D. E. Manolopoulos, "An improved log derivative method for inelastic scattering," J. Chem. Phys. **85**, 6425–6429 (1986).

[61] B. W. Bakr, D. G. A. Smith, and K. Patkowski, "Highly accurate potential energy surface for the He-H_2 dimer," J. Chem. Phys. **139**, 144305 (2013).

[62] J. M. Blatt and L. C. Biedenharn, "The angular distribution of scattering and reaction cross sections," Rev. Mod. Phys. **24**, 258–272 (1952).

[63] M. H. Alexander, P. J. Dagdigian, and A. E. DePristo, "Quantum interpretation of fully state-selected rotationally inelastic collision experiments," J. Chem. Phys. **66**, 59–66 (1977).

[64] M. Jacob and G. Wick, "On the general theory of collisions for particles with spin," Ann. Phys. **7**, 404 – 428 (1959).

[65] W. H. Miller, "Coupled equations and the minimum principle for collisions

of an atom and a diatomic molecule, including rearrangements," J. Chem Phys. **50**, 407–418 (1969).
[66]J. Schaefer and W. A. Lester, "Theoretical study of inelastic scattering of H_2 by Li^+ on SCF and CI potential energy surfaces," J. Chem. Phys. **62**, 1913–1924 (1975).
[67]R. N. Zare, *Angular momentum* (Wiley, NY, 1988).
[68]I. Wolfram Research, "Mathematica online, Version 12.1," Champaign, IL, 2020.
[69]Z. Li, S. V. Alyabyshev, and R. V. Krems, "Ultracold inelastic collisions in two dimensions," Phys. Rev. Lett. **100**, 073202 (2008).